

A photovoltaic degradation evaluation method applied to bifacial modules



Gaetano Mannino ^{a,*}, Giuseppe Marco Tina ^a, Mario Cacciato ^a, Lorenzo Todaro ^b,
Fabrizio Bizzarri ^b, Andrea Canino ^b

^a DIEEI, University of Catania, 95124 Catania, Italy

^b Enel Green Power SpA, Viale Regina Margherita, 125, 00198 Rome, Italy

ARTICLE INFO

Keywords:

Photovoltaics
Bifacial modules
PV degradation
Performance evaluation
Performance Loss Ratio
PV degradation trend

ABSTRACT

The need to replace fossil energy sources with renewable energy sources to combat global warming has prompted the growth and development of various technologies, including photovoltaics. At the same time the PV technology is evolving to enhance efficiency and durability of PV modules. Bifacial PV modules is gaining larger share of market due to the higher energy and power density at almost the same price of conventional PV modules.

In recent years, as PV systems have been operating for a long time, understanding the aging phenomenon of PV modules has become increasingly important. Various types of defects are known that occur during the life of the modules, however, understanding the trend of degradation through a simple quantification of the decrease in performance over time can be a useful tool. The Performance Loss Ratio can give indications about the state of health of the system and can be used for a rough comparison on the performance reduction guaranteed by the module manufacturer and check if the warranty terms are actually respected.

In the present study a simple method is used to evaluate Performance Loss Ratio (PLR) on a real PV plant equipped with bifacial PERC modules.

Criticalities were highlighted within each phase of the application of the method. The numerical results of the PLR estimate of the photovoltaic modules of the system are reported, calculated on a two-year dataset starting from the date of installation. Finally, the PLR values, that have been estimated using three different metrics and linear fitting, have been compared with the measured average Power decay values associated exclusively with PV modules.

The simplicity of the method allows it to be replicated to other case studies.

1. Introduction

Over the past decade, the price of crystalline silicon (c-Si) PV modules has dropped significantly thanks to cost reductions in solar cells, encapsulation, metallisation and assembly. In general, higher performance, better safety and durability combined with a longer lifetime are the ultimate goals of the PV industry.

The proposal of a bifacial c-Si PV module seems to be one of the solutions (Gu et al., 2020). To convert the Irradiance that hits the front and back of the modules, the Bifacial PV modules can use different cell technologies and different packaging design as glass/glass (G/G) or glass/transparent backsheet (G/TB). The bifacial and double glass design has the advantage of power generation on both sides of the module and the modules seem more resistant to environmental factors such as wind, humidity and temperature fluctuations, so more and more

people are willing to install the bifacial modules. According to forecasts, the market share of bifacial modules will continue to increase dramatically over the next 10 years - from 50 % in 2021 to 85 % in 2032 - and the production of traditional monofacial PV cell concepts is likely to be phased out during this period (VDMA, 2020). From technological point of view there is an increasing interest in testing the different solutions regarding not only the technology of the bifacial PV cells but also of the encapsulant and back layer material. As the new solar cell technologies the tunnel oxide passivated contacts (TOPCon), and the Si heterojunction (HJT) have been transferred from the laboratory to production, experimental studies have been conducted on the energy yields of bifacial TOPCon PV modules compared to bifacial HJT and passivated emitter rear contact (PERC) ones, e.g. in (Wang et al., 2022) in Hainan, China, where an experimental field comparison was conducted, it was found that the bifacial HJT module has the highest energy yield among the bifacial TOPCon and PERC modules, 8.85 % compared to the PERC

* Corresponding author.

E-mail address: gaetano.mannino@phd.unict.it (G. Mannino).

Nomenclature	
I_{dc}	Measured Direct Current [A]
V_{dc}	Measured Direct Current Voltage [V]
P_{dc}	measured DC Power [W]
P_{stc}	Power at STC [W]
P_T	Power corrected to STC [W]
$G_{f,POA}$	Front plane of array Irradiance [W/m^2]
$G_{r,POA}$	Rear plane of array Irradiance [W/m^2]
β	Bifaciality factor
γ	Thermal coefficient for Power
T_c	PV cell temperature [$^\circ\text{C}$]
T_m	PV module temperature [$^\circ\text{C}$]
T_{stc}	Temperature at STC, 25°C
G_{stc}	Irradiance at STC, $1000 \text{ W}/\text{m}^2$
P_{norm}	Normalized Power
PR	Performance Ratio
PR_i	Initial Performance Ratio
PR_f	Final Performance Ratio
PR_T	Temperature corrected Performance Ratio
$PR_{T,b}$	Temperature corrected bifacial Performance Ratio
<i>List of abbreviations</i>	
PLR	Performance Loss Ratio
STC	Standard Test Conditions
MPPT	Maximum Power Point Tracking

modules, with most of the contribution due to the high bifaciality and low temperature coefficient. The result shows that TOPCon has a 5.55 % higher energy yield than PERC modules and performs better in low light and high ambient temperatures.

Even if G/G construction promises greater mechanical strength and reduced moisture and weather penetration, older generations of G/G modules containing (polyethylene-co-vinyl acetate) (EVA) suffered from the inclusion of degradation products of the encapsulation (e.g. acetic acid), which in the past led to discolouration of the encapsulation, delamination of the packaging and corrosion of the metallization (JinkoSolar, 2020).

These degradation processes could be mitigated by using higher quality formulations, other encapsulation materials, e.g. polyolefins [POE], or to some extent by using TBs that allow degradation products to diffuse out. G/TB designs also promise lower module operating temperatures, lighter weight (i.e. easier installation) and reduced susceptibility to some types of potential-induced degradation (PID).

However, while the quality of the solar glass is already well established, TB materials suffer from the aging phenomenon and loss of optical transmittance, although TB materials could potentially be improved through appropriate material design. In (Sulas-Kern et al., 2021), several PID and moisture degradation modes are demonstrated to strongly affect EVA-containing modules, with previously reported PID processes under negative bias DH and a unique observation of back surface recombination in G/EVA/G modules under positive bias DH. Significantly less degradation was also observed in POE-containing modules, with the G/POE/G configuration showing minimal degradation under all stress conditions we used.

The CoOs (Cost of Ownership) of bifacial PV modules depends on the adopted technology, in fact, the PERC has almost the same values, that is 9–11¢, whereas others (nPERT, TOPCon and SHJ), with higher bifaciality factors, have increasing CoO values per cell till 18–22¢ (Kopecek and Libal, 2021).

Despite the higher (CoO) of bifacial modules compared to monofacial, the LCOE (Levelized Cost of Energy) seems to favor bifacial photovoltaics due to the higher energy gain thanks to the absorption of Irradiance also from the back of the module. However, LCOE is strongly influenced by the energy generated by the PV system throughout its lifetime, so the useful life of the PV system is extremely important for the precision LCOE calculation. The useful life of the PV modules is defined as the time in which they are able to maintain the efficiency not below 80 % of the rated one, in the last decade the guaranteed useful life period passed from 25 to 30 years. Furthermore, the PV module manufacturers guarantee a degradation trend, often linear and expressed in %/y, which will not be exceeded. The degradation rate of the photovoltaic modules, to fall within the warranty terms, should therefore be below 0.8 %/year.

As monofacial PVs were marketed much earlier than bifacial, data on their degradation rate are widely available. In (Jordan and Kurtz, 2013), the values of the degradation rate per year for different photovoltaic

technologies are reported; regarding silicon-based technologies the average degradation rate per year is approximately 0.36 % for mono-crystalline silicon and 0.64 % for multi-crystalline silicon. However, in (Kim et al., 2021) is reported a list of cases of PV plants equipped with Multi-Si Solar Cell and exposure times of more than 10 years in various countries, the degradation rates are higher than 0.8 % and most of the degradation is caused by environmental conditions, such as high humidity, extreme ambient temperatures. The study (Jordan et al., 2022) based on datasets from PV plants located in the USA, both commercial and utility scales, for a cumulative capacity greater than 7 GW, recorded the median of the PLR equal to $-0.75\%/\text{y}$. In (Theristis et al., 2022) the degradation of recent photovoltaic module technologies is analyzed, highlighting that out of 23 systems, 6 will fail to meet the warranty terms. Some studies as (Bouaichi et al., 2020; Silvestre et al., 2018) have shown that in extreme conditions, under high temperatures and irradiances as in desert environment, the overall degradation can vary depending on PV technology, and can greatly exceed the warranty terms (Bouraiou et al., 2017). Depending on the mechanism involved, the degradation of solar panels in the field can be long-term or short-term; considering that the degradation might increase over time, still insufficient failure data are currently available for “end of life” statistical analyses as most operating PV modules have not yet reached 25 years of operation (Sulas-Kern et al., 2021). The factors and mechanisms underlying degradation are well known, in operation, PV modules are subject to constant cycles of temperature, humidity, irradiation, mechanical stress and soiling, which can lead to defects and diverse degradation phenomena such as encapsulant yellowing, microcracks, metal contacts detaching, breaking and rusting, light-induced degradation, and potential induced degradation (da Silva et al., 2021). It is important to have a deep understanding of the degradation rate as it can eventually lead to module failure or, in case of the underestimation of the degradation rate, lead to an increase in the financial risk (Liang et al., 2019). In addition to material degradation, a PV module is exposed to other factors in outdoor conditions that directly affect its electrical performance. These include diffuse soiling, snow, shading, module and cell mismatch.

For the purposes of this study, it is therefore more appropriate to refer to the power loss rate (PLR) rather than the degradation rate (DR). The PLR includes reversible and irreversible power loss, the DR only irreversible power loss. Without monitoring the pollution effect and without a register of maintenance interventions, it is difficult to distinguish whether the performance degradation is reversible or irreversible, so the PLR is analyzed in this study. Indoor and outdoor measurements can be used to evaluate PLR. For the latter, the electrical parameters can be recorded in special test facilities built mainly for research purposes and equipped with I/V curve meters that collect data at a frequency of at least 10 min (Tina et al., 2016). Some companies recently started to offer on the market sensors able to detect the I/V curves at the module level. Another category of outdoor measurements involves the use of electrical

recordings from modules held continuously at the Maximum Power Point (MPP), also using commercial inverters (Spataru et al., 2016). This last type of study is of particular interest to plant owners and installers, as it can be performed for any type of PV plant connected to the grid, provided that a reliable irradiance measurement is available.

In general, the calculation of PLR using field measurements requires the introduction of a performance metric and a statistical method. The first consists of an analytical technique for calculating representative performance estimates on a selected time scale (usually monthly). Among these, the array performance ratio (PRA) index is one of the most commonly used for outdoor measurements (Kunaifi et al., 2020; Carigiet et al., 2021). The statistical methods are mathematical algorithms applied to the time series of performance estimators to extract a trend. Linear regression is one of the most common, but classical series decomposition, locally weighted scatter plot, smoothing and autoregressive integrated moving average are also used; in (Abdelouahed et al., 2022) different statistical techniques are described.

The accuracy of PLR calculation depends on the combination of performance measure, filtering techniques and statistical methods used to succeed in minimizing seasonal fluctuations and eliminating outliers (Lindig et al., 2021). This paper therefore applies a PLR calculation procedure based on the use of the array PR metric in combination with an appropriate filtering technique and linear regression, with the aim of reducing the overall uncertainty in the estimation of PLR. The study is conducted on bifacial PERC-PV technologies and considers two years of operational data of the bifacial PV plant.

2. Method and background

In the present study, a step-by-step method for PLR estimation similar to the one presented in (Lindig et al., 2022) is used. The steps necessary to determine the PLR are shown in Fig. 1.

After the graphic display of all the quantities within a dashboard that represents them all at the same time, the dataset is classified, and the initial cleaning of the data takes place. The choice of the metric has been proposed before the application of the Irradiance filter because it is applied mainly according to the installation site of the system but also according to the metric used; for example, if the normalized power is used as a metric, it would be useful to choose a narrow Irradiance filter and, if possible, close to the STC so that the P_{norm} is less variable. After the application of the Irradiance filter, an additional filter is applied (in the case study the PR is used as filter), and finally the estimate of the Performance loss ratio is performed on the filtered quantities.

3. PV system description

The PV system consists of 7 bifacial PERC photovoltaic modules connected in series, the Nominal Power of each module is equal to 370 W, the Nominal Power of the system is 2590 W. The DC Current and DC Voltage of the string are acquired with a Current transducer and a Voltage transducer respectively. The Front Irradiance is acquired through a class A Pyranometer on the same plane of the array, the ambient temperature through a Thermohygrometer located in the same

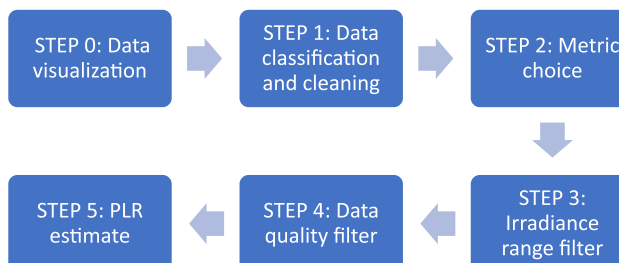


Fig. 1. PLR estimation steps.

site, the module temperature through a PT100 located on the back of one of the central modules. The Rear Irradiance hitting the modules is acquired through a reference cell located on the back of another PV plant which is 2.6 m away from the analyzed system. The PV plant that is equipped with the reference cell on the back has: the same structure and configuration, the same tilt angle of 37.5° and it is located on the same type of ground. Therefore, for the purpose of this study, it is assumed that the Rear Irradiance is the same as that of the analyzed PV plant. Front and back sides of the PV system are shown in Fig. 2 and Fig. 3, the monofacial modules located at the top of the string are part of another PV system, one of the upper external bifacial modules is not connected.

4. Step by step method and application to bifacial PV plant

The estimated PLR is caused by the decrease in the performance of the entire system, which is made up of numerous components that deteriorate and affect the overall performance. However, in order to understand the trend of module degradation, and not having precise information on the performance of the various components, in this study the decrease in PLR is attributed only to the PV modules. Electrical and environmental data available for the PV plant and site of installation have been acquired for a period of 2 years with 1 min sampling resolution.

STEP 0: Data Visualization

Before proceeding with data analysis, it is of fundamental importance to check the availability and reliability of the data. It is useful to plot each acquired quantity to qualitatively inspect the dataset.

The data visualization is a qualitative tool that helps to:

- Check if the data have a uniform timestamp and verify that all the variables are synchronized.
- Identify missing data for each quantity
- Visualize if some variables are missing in different time periods from each other.

Using the matlab “stackedplot” graph it is possible to represent all the variables of a dataset as shown in Fig. 4.

From top to bottom, the acquired quantities are as follows: string AC Voltage, string AC Power, string DC Voltage, string DC Current, AC Current, Irradiance on the module surface, Irradiance on the back of the modules, ambient Temperature, module Temperature.

There are periods in which the data have not been acquired, where the signal is missing or where it remains constant (Fig. 4); where the signal is missing it will be removed with the method presented in the next paragraphs, where it is constant instead it is removed using other different filters as the variable changes. The Irradiance values that are



Fig. 2. PV system, PERC bifacial modules. Front side.



Fig. 3. PV system, PERC bifacial modules. Back side.

used in the analysis are in defined and positive ranges, all other values will be removed.

Data Visualization allow to see if there are out-of-scale values for each acquired quantity, for each quantity the outliers that stray too far from the scale can make it more difficult to visually inspect the consistency of the quantity with the measurement scale. This in the case study this occurs in the case of AC Voltage both in the first and in the second year. However, it is advisable to repeat the visual inspection step even after filtering the data.

STEP 1: Data classification and cleaning

Before proceeding with the analysis about PLR estimation, it is necessary to identify which are the missing variables among those acquired, and when they are missing.

It would be necessary to proceed for each variable and keep track of the missing data and the timestamp.

Subsequently, based on the amount of missing data for each variable, it is possible to:

- Remove all the data in the periods in which a certain variable was missing
- To model the determined variable through specific models
- To insert data by interpolation in place of the missing samples for that given variable.

In (Lindig et al., 2021; Lindig et al., 2022) a method of data evaluation is proposed by assigning a letter that identifies the quality of the dataset (see Table 1):

A period of at least two years is necessary to assess degradation. In the analyzed case study, as it is possible to see in Fig. 4, most of the missing variables are missing at the same time. Therefore, by selecting a variable, in this case the string DC Current, it is possible to identify the missing samples also for the other variables. Fig. 5 and Fig. 6 show the DC current acquired respectively for the first and the second year.

In the period between 01/08/2020 and 31/07/2021 there are 74,669 missing out of 524,160 samplings (364 days), most of which grouped into macro-periods, therefore equal to approximately 14 % of the total samples.

In the period between 01/08/2021 and 31/07/2022 there are 18,024 out of 524,160 samplings missing, most of which grouped into macro-periods, equal to about 3.5 % of the total samplings.

However, there are visibly incorrect data, which are close to the null value, but which are not reported as missing. Since the wrong values of the measured quantity could vary and, at the same time other quantities could be acquired correctly, the wrong values of the specific quantity (in this case DC current) will be identified and excluded from the PR filter

Table 1
Data quality grading scheme (Lindig et al., 2022).

Letter Grade	Outliers (%)	Missing percentage (%)	Longest gap (days)
A	Below 10	Below 10	Below 15
B	10–20	10–25	15–30
C	20–30	25–40	30–90
D	Above 30	Above 40	Above 90
P/F	Time series \geq 24 months	= >Pass	

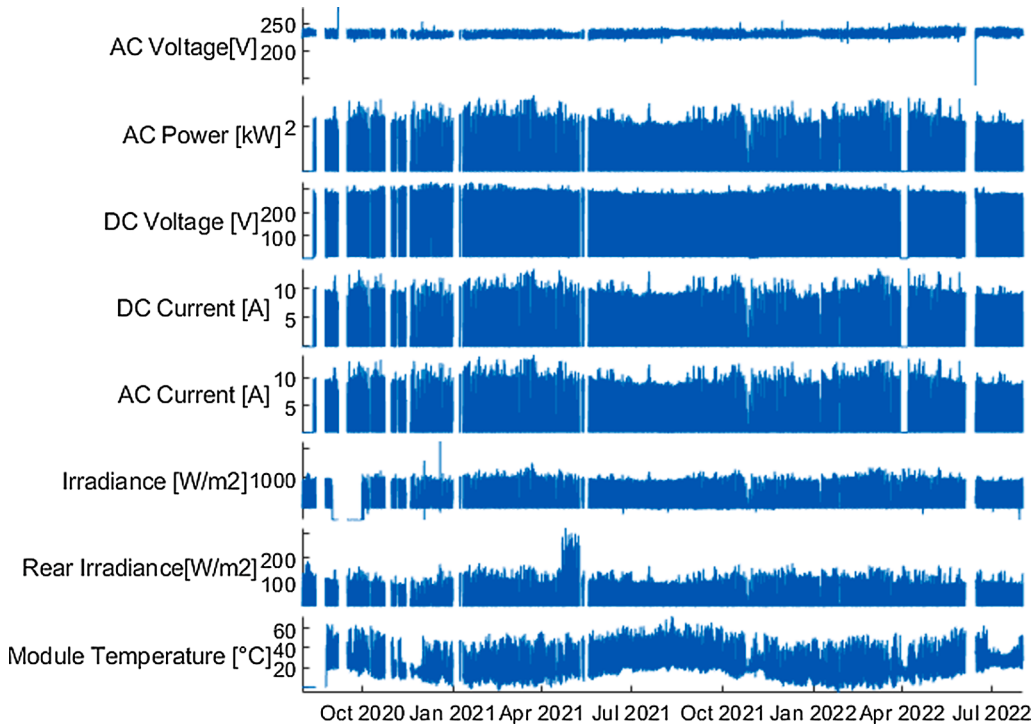


Fig. 4. Acquired Data, period 01/08/2020–31/07/2022.

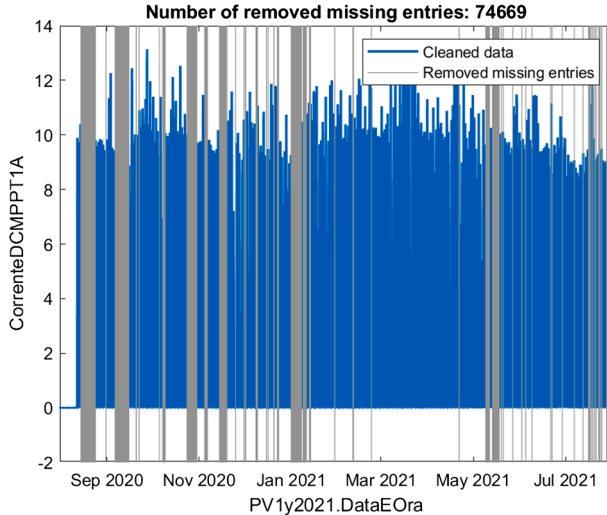


Fig. 5. PV string DC Current, year 2020–2021.

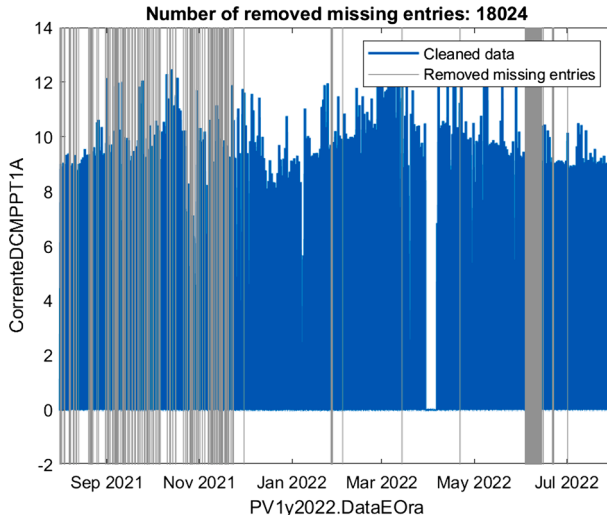


Fig. 6. PV string DC Current, year 2021–2022.

that will be applied in the following steps.

As highlighted in (Lindig et al., 2021; Lindig et al., 2022), for the dataset to fall into class A, the number of missing samples should be less than 10 %, however no indications are given on the temporal distribution of the missing data (only about the longest gap), and on how it affects the analysis of the PLR.

In (Romero-Fiancés, 2022) the influence of missing data in the degradation analysis is analyzed. In the present study, the lack of data is simply checked year-by-year; once the missing data have been identified, all data are removed for the same period in which the reference variable (in this case I_{DC}) is missing.

STEP 2: Metric choice

Normalized Power (P_{norm}), Performance Ratio (PR), Temperature corrected Performance Ratio (PR_T), and Temperature and Rear Irradiance corrected Performance Ratio (PR_{Tb}) can be used as metrics to identify the Performance Loss Ratio:

$$P_{norm} = \frac{P_{dc}}{P_{stc}} \quad (1)$$

Where P_{dc} is the measured DC Power [W] and P_{stc} is the Power at STC [W]

$$PR = \frac{\frac{P_{dc}}{P_{stc}}}{\frac{G_{f,POA}}{G_{stc}}} \quad (2)$$

Where $G_{f,POA}$ is the front plane of array Irradiance [W/m^2] and G_{stc} is the Irradiance at STC ($1000 \text{ W}/\text{m}^2$)

$$P_T = P_{dc} \frac{G_{f,POA}}{G_{stc}} \frac{1}{[1 + \gamma(T_c - T_{stc})]} \quad (3)$$

Where γ is the thermal coefficient for Power, T_c is the PV cell temperature [$^\circ\text{C}$] and T_{stc} is Temperature at STC (25°C)

$$PR_T = \frac{\frac{P_{dc}}{P_{stc}[1+\gamma(T_c-T_{stc})]}}{\frac{G_{f,POA}}{G_{stc}}} \quad (4)$$

$$PR_{Tb} = \frac{\frac{P_{dc}}{P_{stc}[1+\gamma(T_c-T_{stc})]}}{\frac{G_{f,POA}+\beta G_{r,POA}}{G_{stc}}} \quad (5)$$

where $G_{r,POA}$ is the rear plane of array Irradiance [W/m^2] and β is the bifaciality factor.

The simplest metric is the P_{norm} in Eq. (1), in the presence of sufficiently long datasets it is possible to use it to identify a trend for the PLR since the output power from the system decreases over the years; however, it is the metric that suffers the most variability and therefore gives greater uncertainty in the PLR estimate.

The PR in Eq. (2) is commonly used as metric, both for performance evaluation and for PLR estimation. PR can be calculated using DC or AC electrical data, however using DC data gives the advantage that Inverter performance losses are excluded (assuming the functioning of the MPPT unchanged over time). As example the study (Quansah and Adaramola, 2019) adopted the classical PR as metric for the early PV degradation assessment.

In (Belluardo, 2015) the method is based on the estimation of monthly averages of array generated Power corrected to STC conditions (3), such metric is used also in (Subramanyan et al., 2018) in order to evaluate the degradation of a PV plant to build a PV degradation forecast model. In (Jordan et al., 2017) a methodology that use Eq. (4) as metric was applied to a fleet of PV systems, such metric coupled with different filtering steps was able to discriminate between the long-term degradation behavior of different technologies. Eq. (5) is similar to Eq. (4) but suitable for bifacial because the irradiation on the back of the modules and the bifaciality factor of the modules are considered. It is possible to find the Eq. (5) in IEC 61724-1:2021 with different nomenclature (IEC 61724-1: 2021).

The classical PR, the PR_T and the PR_{Tb} are adopted to calculate the PLR over two years.

For simplicity of calculation, the module temperature value is entered in Eqs. (4) and (5) instead of cell temperature. However, the cell temperature value is generally close to the module temperature value; according to (King et al., 2004) the temperature difference between the cell and the module back surface at an irradiance level of $1000 \text{ W}/\text{m}^2$ is typically $2\text{--}3^\circ\text{C}$ for flat-plate modules in an open-rack mount. Also, in (Piliouguine et al., 2021) experimental results show that the mean value of difference between cell temperature and module temperature was 2.5°C and the associated standard deviation from the mean value was 0.52°C . As stated in (Tina et al., 2020) can be noted that the temperature of the back glass module is very close to the cell temperature, even it depends on environmental and operational condition.

In the case study are used only experimental data, without using modeled variables. Further studies could analyze the impact to the final results by using modeled variables supporting missing data or instead of experimental acquired variables. The choice of the metric used is proposed in this section because the filtering methods can be chosen taking into account the metric that will be used.

STEP 3: Irradiance range filter

The choice of the irradiation range which to consider the data, within

an analysis is of fundamental importance. As expanding the irradiation range means to consider the response of the PV system in different conditions, which can prove to be an advantage as stated in (Lindig et al., 2022); but using PR; PR_T , and P_{norm} as a metric, the variability of these values increases during the day, making long-term analysis more difficult. Since the purpose of this study is to identify the degradation trend of the plant, in this analysis the narrow range close to the standard conditions of 800–1200 W/m² has been chosen, as it has been done in (Makrides et al., 2010).

Another aspect to consider when choosing the irradiation filter are the characteristic values of irradiation of the site where the plant is located, since the analyzed plant is located near Catania, in South Italy, this range allows to have enough data that fall for each month.

It may be useful to know how many samples were in the dataset and how many remain after the application of the radiation filter.

Although there is a data classification upstream of the analysis, it is important that enough data remain once the irradiation filter has been applied. In the case study, after the application of the Irradiance filter, the samples went from 450,871 to 52,511 for the first year and from 507,516 to 63,016 for the second year.

Narrowing the range of the irradiation filter does not exclude conditions that can negatively affect the output power, it is therefore necessary to apply data quality filter as in the following paragraph.

STEP 4: Data quality filter

The PR with one minute resolution is used as a data quality filter, it allows to discard all those data where the electrical and environmental quantities are misaligned. The data quality filter is a tool that allows to avoid errors that occurs during transients, different response times of sensors such as voltage and current transducers with respect to the pyranometer or temporary partial shading phenomena as examples. Furthermore, an extremely high PR value could indicate that the pyranometer is dirty or subject to problems that cause irradiation values to be acquired lower than the real ones, causing the PR value to increase excessively. Conversely, too low values may indicate malfunctions or particularly dirty modules.

Once all the filtering methods have been applied, it is important to consider the number of remaining samples that will be used within the analysis. Using the Matlab “*obscount*” command it was possible to automatically track the number of remaining samples for each month.

As the filtering method for the PR, but also for the other performance metrics as PR_T , the threshold interquartile was used; it is suggested in (Lindig et al., 2021) as the usual method. Quartile filter “Returns true for

elements more than 1.5 interquartile ranges above the upper quartile (75 percent) or below the lower quartile (25 percent)” (GUM – JCGM 100, 2008).

By monitoring the bifacial modules, the PR value is more variable than in the case of monofacial modules, as this value is also affected by the irradiation on the back of the module. When the Rear irradiance is not monitored, it is more difficult to identify the PLR. Therefore, the application of the quartile method with the threshold factor of 1.5 already excludes more values than would be discarded considering monofacial modules, for this reason the threshold factor was set to 4 instead of 1.5. The graphs in Fig. 7 and Fig. 8 report the values of the PR over time over a year, for the range of irradiation 800–1200 W/m². (The samples are graphically connected by a continuous line but only the point values within the irradiation range are used) (see Figs. 7–12).

The identified and eliminated outliers are 3464 the first year and 2052 the second year.

Except for September, when the available data was limited, the number of samples for each month was acceptable (Table 2 and Table 3).

The filtering method has been applied to each year separately, since by applying it to a longer period (2 years or more) if there are significant PLR values, there is a risk of excluding a large part of the dataset at the beginning and/or at the end of the period. Starting from the data already filtered using the PR, the values of PR_T and PR_{Tb} (calculated with a sampling time equal to one minute) must also be filtered to eliminate the outliers which would alter the monthly average values. The same filtering method applied to the PR was therefore applied to the PR_T and PR_{Tb} metrics (Figs. 9–12). Since the new input data has already been filtered by the PR filter, the outliers identified by applying the filter for the PR_T and PR_{Tb} metrics will be less than those identified by the PR filter. In this study the threshold factor that is used for the PR_T and PR_{Tb} filtering is the same of the one used for the PR; however, it may be useful to increase it for the PR_T and PR_{Tb} . The filter range is not a trivial choice, since if it is too wide, there is the risk of considering outliers as significant samples, while if it is too narrow, there is the risk of excluding significant data.

STEP 5: PLR estimate

The proposed metrics P_{norm} , PR, P_T , PR_T , PR_{Tb} can be used as metric. The P_{norm} is the most variable of the four listed, the PR is less variable than the P_{norm} because the PR considers the Irradiance, but it is more variable than PR_T and PR_{Tb} because it does not take into account the module temperature and Irradiance on the back of the module.

In this case study, the metrics PR, PR_T and PR_{Tb} have been applied to

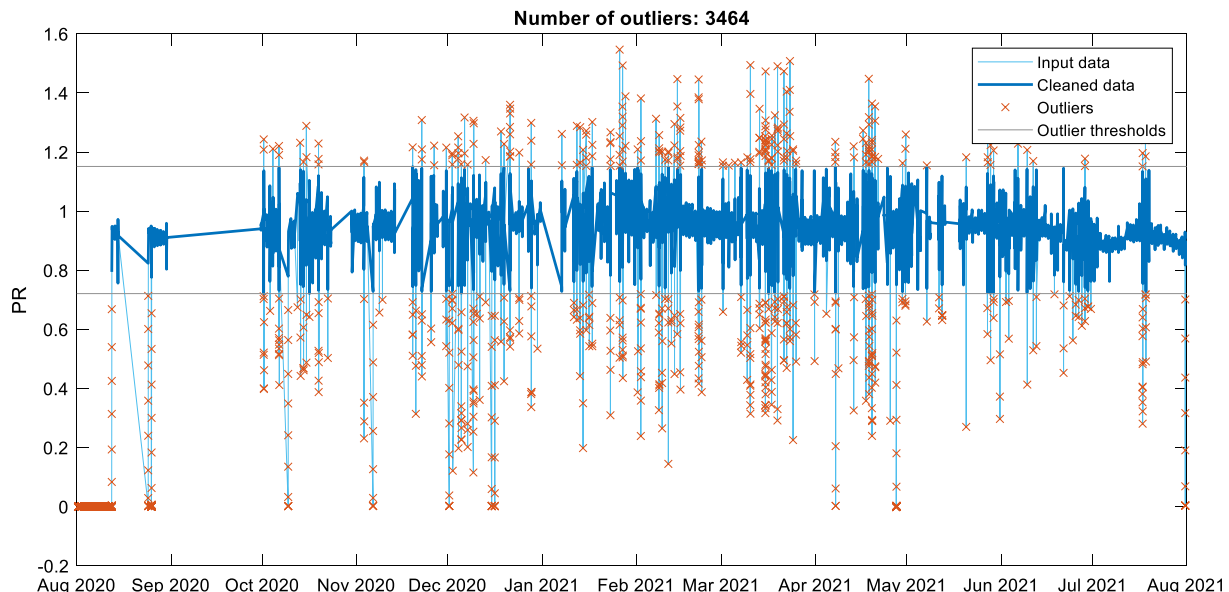


Fig. 7. Filtered PR for Irradiance range input 800–1200 W/m², period 01 Aug 2020–31 July 2021.

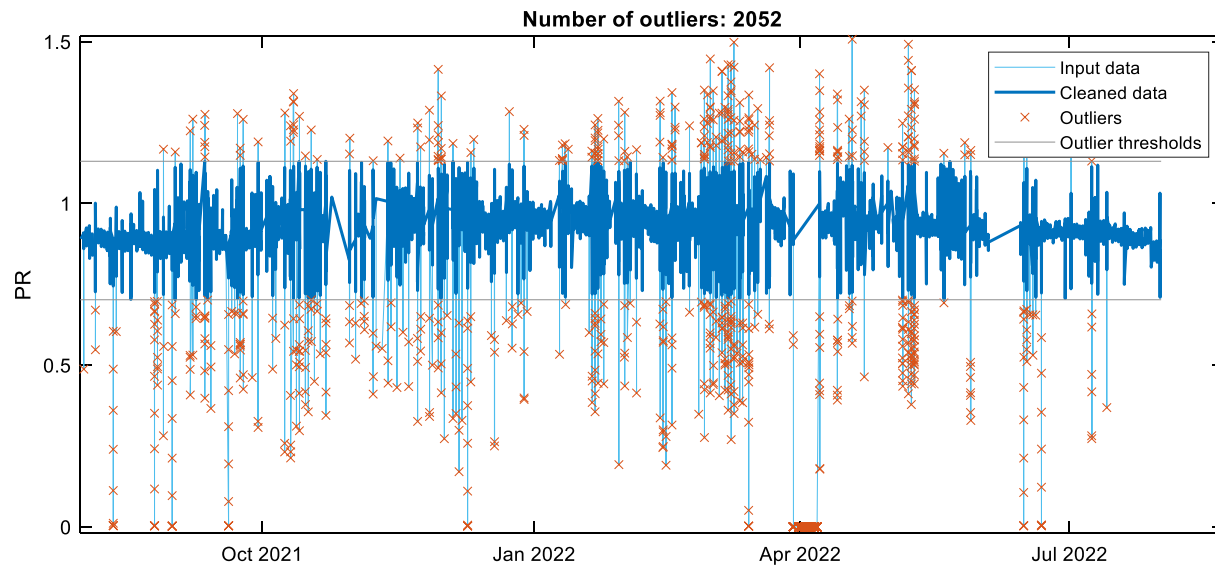


Fig. 8. Filtered PR for Irradiance range input 800–1200 W/m², period 01 Aug 2021–31 July 2022.

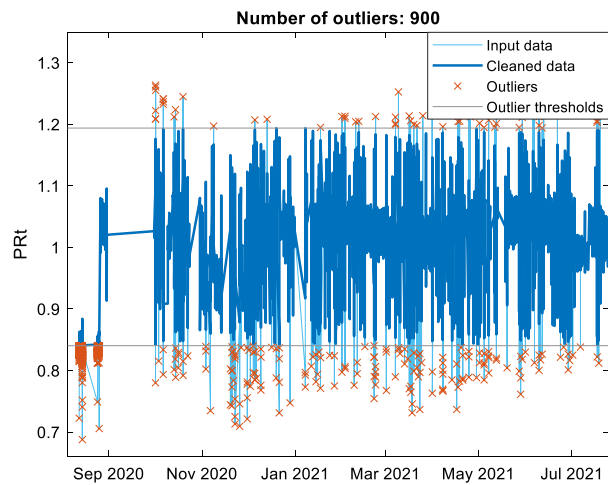


Fig. 9. Filtered PR_T for Irradiance range input 800–1200 W/m², period 01 Aug 2020–31 July 2021.

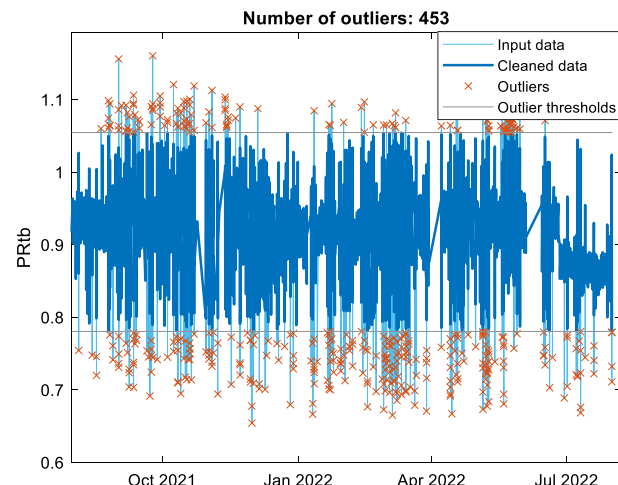


Fig. 11. Filtered PR_{Tb} for Irradiance range input 800–1200 W/m², period 01 Aug 2020–31 July 2021.

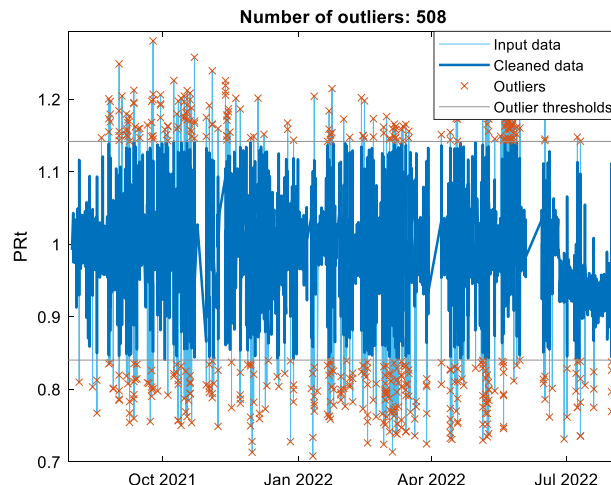


Fig. 10. Filtered PR_T for Irradiance range input 800–1200 W/m², period 01 Aug 2021–31 July 2022.

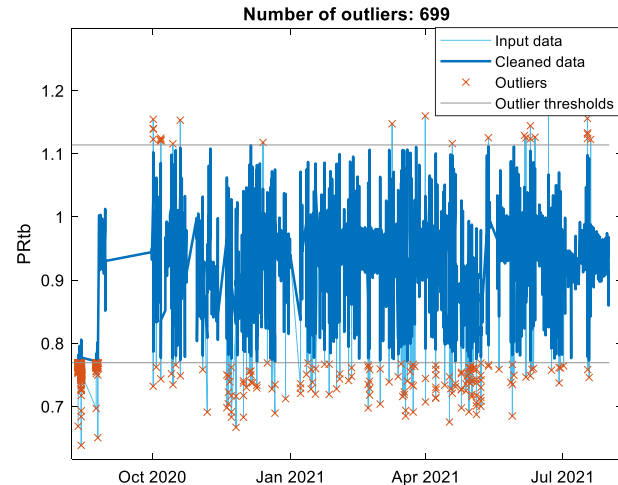


Fig. 12. Filtered PR_{Tb} for Irradiance range input 800–1200 W/m², period 01 Aug 2021–31 July 2022.

Table 2

Number of samples considered per month, period 01 Aug 2020–31 Jul 2021.

Year	2020					2021						
Month	Aug	Sep	Oct	Nov	Dec	Jan	Feb	Mar	Apr	May	June	Jul
Sample number	2370	23	4148	3286	3691	2017	6027	5706	5140	4487	5213	6939

Table 3

Number of samples considered per month, period 01 Aug 2021–31 Jul 2022.

Year	2021					2022						
Month	Aug	Sep	Oct	Nov	Dec	Jan	Feb	Mar	Apr	May	June	Jul
Sample number	7081	6241	3477	2949	4069	4707	6167	4115	4906	6075	4080	7097

a data acquisition period of two years. The PR, PR_T and PR_{Tb} values, within the selected Irradiance range, have been grouped within each month and the average has been calculated. The monthly average value of the PR, PR_T , PR_{Tb} during the first and second year in which the plant was monitored are represented respectively in Fig. 13 and in Fig. 14.

$$y = ax + b \quad (6)$$

Where y represent the modeled performance metric used for PLR calculations at the x month. The regression parameters, a and b , are obtained by applying the model to the experimental data, a and b will be associated to the specific metric adopted to calculate the PLR.

Using a generic metric (M) it is possible to calculate the PLR for one year using the following equation:

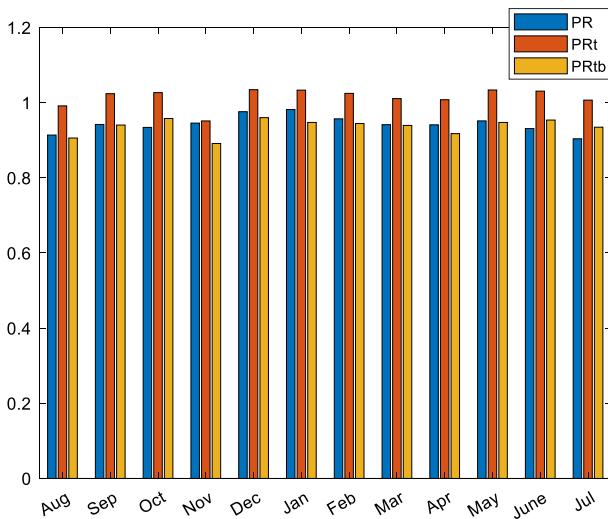
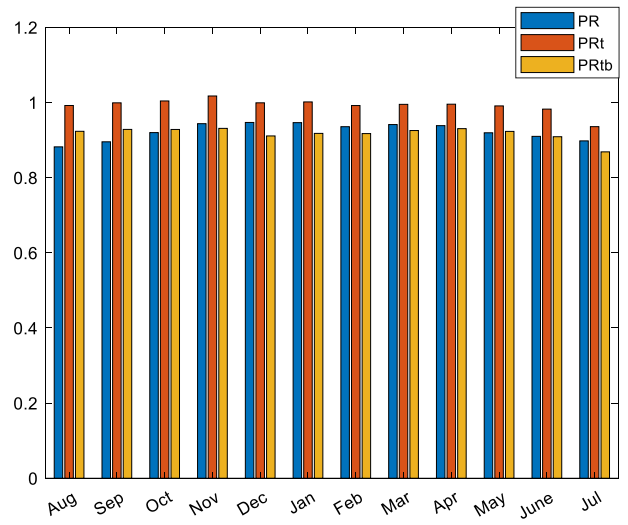
$$PLR(M) = \frac{M_{final} - M_{initial}}{M_{initial}} = \frac{12a + b - b}{b} = \frac{12a}{b} \quad (7)$$

Where M_{final} is the estimated value of the metric at the end of the period and $M_{initial}$ is the estimated initial value of the metric. As example, using the PR as a metric it is possible to calculate the PLR for one year through the simple equation (8):

$$PLR(PR) = \frac{PR_f - PR_i}{PR_i} = \frac{12a_{PR} + b_{PR} - b_{PR}}{b_{PR}} = \frac{12a_{PR}}{b_{PR}} \quad (8)$$

Eq. (6) can be used also for different time-period by inserting the months number instead of x .

It is possible to calculate the uncertainty associated with the estimate of the PLR, as carried out in (Belluardo, 2015) through the Eq. (9) (GUM – JCGM 100, 2008):

Fig. 13. Monthly average PR, PR_T , PR_{Tb} period Aug 2020–Jul 2021.Fig. 14. Monthly average PR, PR_T , PR_{Tb} period Aug 2021–Jul 2022 To evaluate the Performance Loss Ratio, a linear regression model is applied.

$$u_{PLR} = \sqrt{\left(\frac{\partial PLR}{\partial a}\right)^2 \cdot u_a^2 + \left(\frac{\partial PLR}{\partial b}\right)^2 \cdot u_b^2} \quad (9)$$

$$\frac{\partial PLR}{\partial a} = \frac{12}{b} \quad (10)$$

$$\frac{\partial PLR}{\partial b} = -\frac{12a}{b^2} \quad (11)$$

$$u_{PLR} = \sqrt{\left(\frac{12}{b}\right)^2 \cdot u_a^2 + \left(\frac{12a}{b^2}\right)^2 \cdot u_b^2} \quad (12)$$

u_{PLR} , u_a and u_b are the standard deviations associated to PLR, a and b , respectively. The error between the estimated linear model Metric and the measured Metric, is computed as:

$$\varepsilon_x = M_{est,x} - M_{meas,x} \quad (13)$$

using the PR metric as example, the Eq. (13) would be:

$$\varepsilon_x = PR_{est,x} - PR_{meas,x} \quad (14)$$

where x is the x th month to which the monthly average PR refers.

The error ε_x is assumed normally distributed as in (Belluardo, 2015), therefore it is possible to calculate the standard deviations associated to the linear regression coefficients, a and b , respectively:

$$u_a^2 = \sigma_a^2 = \frac{\sum_{x=1}^N (\varepsilon_x)^2}{N - 2} \cdot \frac{1}{\sum_{x=1}^N (t_x - \bar{t})^2} \quad (15)$$

$$u_b^2 = \sigma_b^2 = \frac{\sum_{x=1}^N (e_x)^2}{N-2} \cdot \left(\frac{1}{N} \cdot \frac{\bar{t}^2}{\sum_{x=1}^N (t_x - \bar{t})^2} \right) \quad (16)$$

where N is the total number of months and \bar{t} is defined by Eq. (13):

$$\bar{t} = \frac{\sum_{x=1}^N (t_x)}{N} \quad (17)$$

By substituting the coefficients, a and b, obtained from the linear fitting applied to a two-year period, the PLR values are detected. The linear regression model is applied to the monthly mean PR, PR_T and PR_{Tb} values during the two years in which the plant was monitored.

The linear fitting of the monthly average PR, PR_T , PR_{Tb} and the equations with the relative a and b coefficients are shown, respectively, in Fig. 15 Fig. 16 and Fig. 17.

There is a strong fluctuation of the monthly PR values (Fig. 15), this is due to the fact that the following effects on the decrease of the power are not considered: cell temperature and the soiling. Furthermore, extremely high temperatures were recorded in August 2021; In Ragusa, a city in the same region of the PV system, the temperature record for Europe was broken, equal to 48.8 °C on 11 August 2021.

The irradiance on the back of the modules is a further source of fluctuation, even if it is limited because the 800–1200 W/m² Irradiance range filter has been applied.

The correction with respect to the temperature compensates for the effect of decreasing power due to the increase in temperature, this is evident in the increase in the value of the PR_T in the summer months compared to that of the PR. The correction with respect to the back-module Irradiance is made by applying the PR_{Tb} metric defined in Eq. (5); it takes into account the power gain due to the effect of the surplus of irradiation that affects the back of the module. In Fig. 17 the monthly PR_{Tb} and linear fitting for the two years of acquisition time is represented.

The monthly variation of the PR_T and PR_{Tb} is smaller than that of the

PR, this is due to the correction with respect to the module temperature of the output Power, and in the case of the PR_{Tb} also with respect to the Irradiance hitting the back of the module. However, there is still a variability of the values (both for PR_T and for PR_{Tb}) this could be due to:

- Soiling effect due to severe dirty conditions
- During particularly high temperatures the real thermal coefficient for Power could be different from that provided by the datasheet. The thermal coefficient provided in the datasheets is in fact a linearization of the Power decrease as the temperature increases.

The average values of the used metrics and the number of samples for each month and for each metric are reported in Table 4.

Considering the entire monitoring period, two-year dataset, and applying linear fitting to the monthly average values, a line with a negative slope was obtained (characteristic of a decrease in performance) for the three metrics. Using PR as a metric, it is achieved a PLR of $-1.61\%/\text{y}$, which corresponds to a total PLR of 3.21 %.

Using the PR_T , a value of $1.93\%/\text{y}$ is obtained, which corresponds to a total PLR of -3.85% . Instead, using the PR_{Tb} , the obtained PLR is $1.71\%/\text{y}$, which corresponds to the total PLR of -3.41% . The smallest uncertainty is of the PR_{Tb} , followed by the uncertainty of the PR_T . The uncertainty of the PR is instead the highest. The results of the PLR and the related uncertainty are shown in the Table 5.

5. Results comparison with solar simulator lab test

To verify the effectiveness of the method used to determine the PLR, the estimated PLR was compared with the Power decay recorded in the solar simulator. Although it is not correct to directly compare the PLR with the Power decay, since the PLR includes both reversible and irreversible phenomena, it is still useful to make the comparison to understand how far the PLR estimate is from the real Power loss value of the

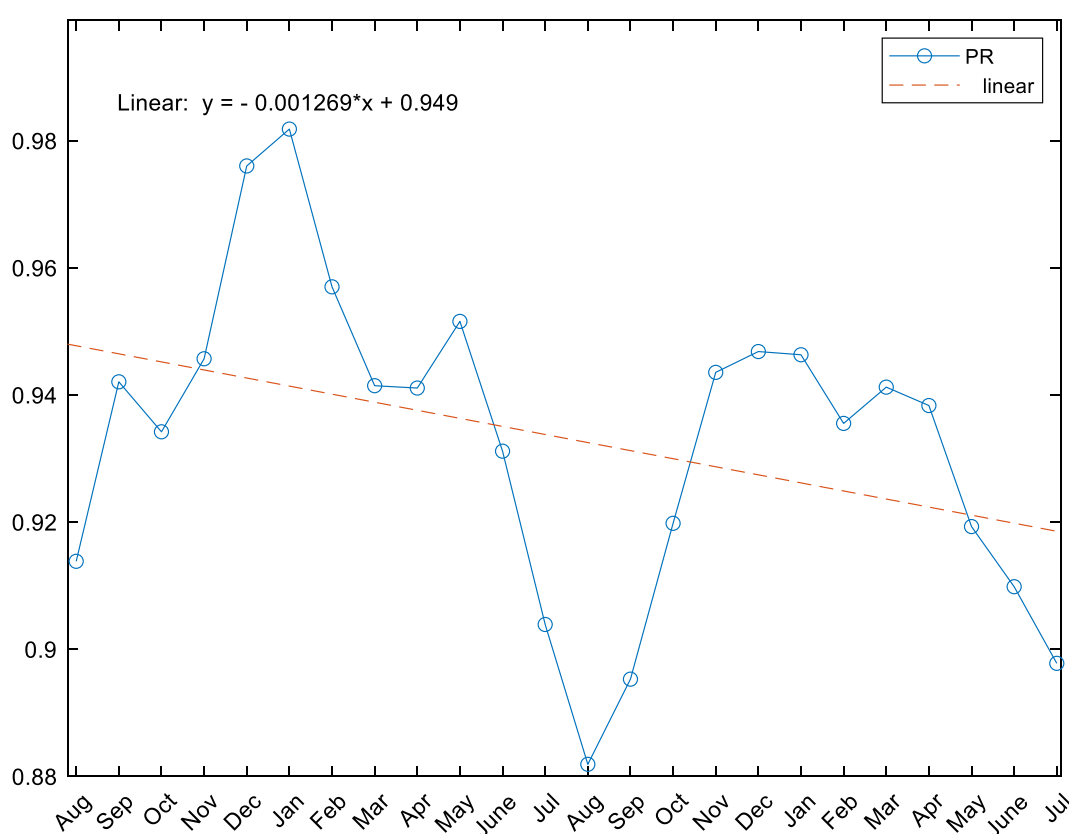


Fig. 15. Monthly PR and linear fitting, period Aug 2020–Jul 2022.

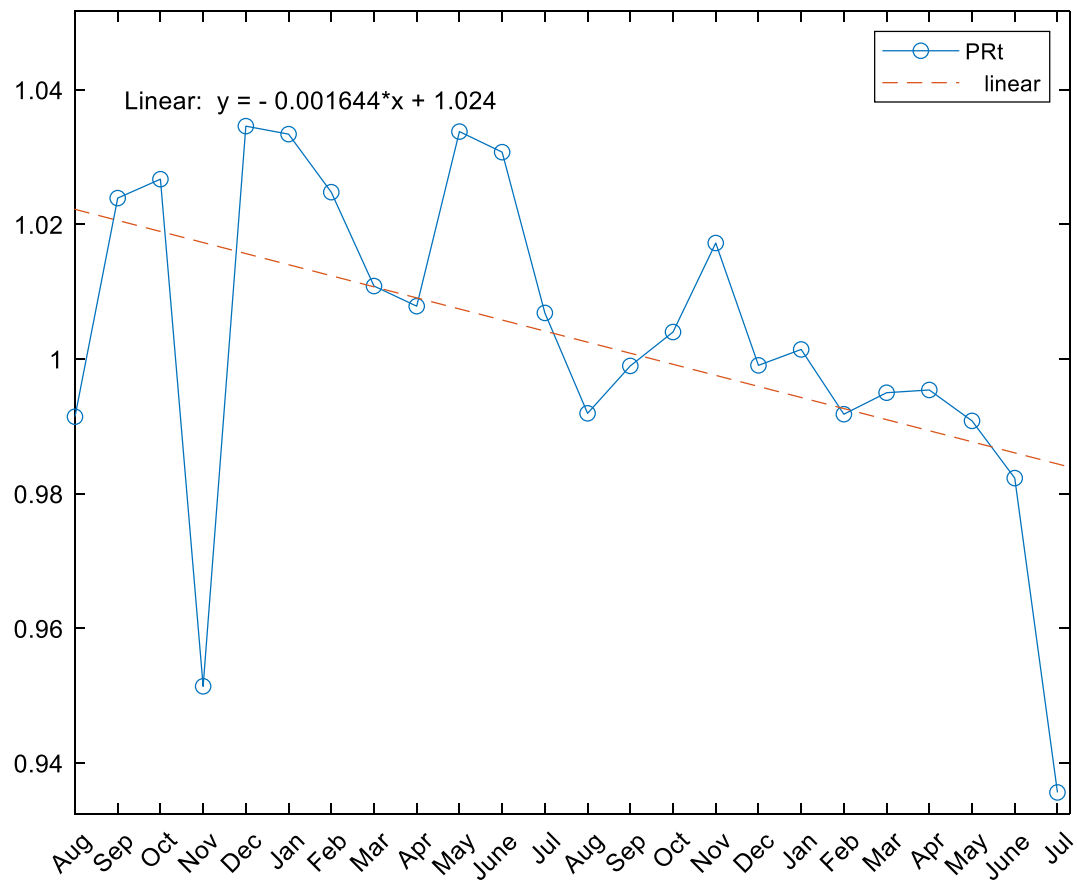


Fig. 16. Monthly PR_T and linear fitting, period Aug 2020–Jul 2022.

PV modules due to degradation.

The PLR can be used as a tool to understand when it is probable that the warranty conditions of the PV modules mounted on the system are not respected; for example, when PLR calculated values deviate much from the warranty terms for Power decay. The confidence limits to determine exactly when the warranty terms of the modules are not met is beyond the scope of this research. However, the high PLR values suggest that it is possible that the modules have undergone a higher degradation process than usual, considering the short exposure time.

The 7 PV PERC bifacial modules of the monitored photovoltaic system were sent to the solar simulator laboratory test. By comparing the tests carried out after the stabilization of the modules (just before installation) with those carried out 19 months after their installation, an average Power decay of 3.35 % was obtained.

Substituting 19 in place of \times in Eq. (6) and applying Eq. (7) a PLR value of -2.54 % is obtained using the PR metric, -3.05 % using the PR_T and -2.70 % using the PR_{Tb}.

The difference between the estimated PLR and the Power decay obtained for a period of 19 months is therefore equal to 0.81 %, 0.3 % and 0.65 % respectively using the PR, PR_T and PR_{Tb} metric. Despite the linear interpolation model applied to outdoor data, that was performed over 24 months (and therefore influenced by 5 months more than the time when the solar simulator tests were carried out) it was possible to obtain PLR values not so far from the Power decay actually suffered by the modules.

The accuracy of the results obtained from the model applied in this work can be improved upstream by:

- PV system maintenance plan and soiling monitoring
- Active control of the acquired variables both electrical and environmental so that the initial dataset could be more affordable

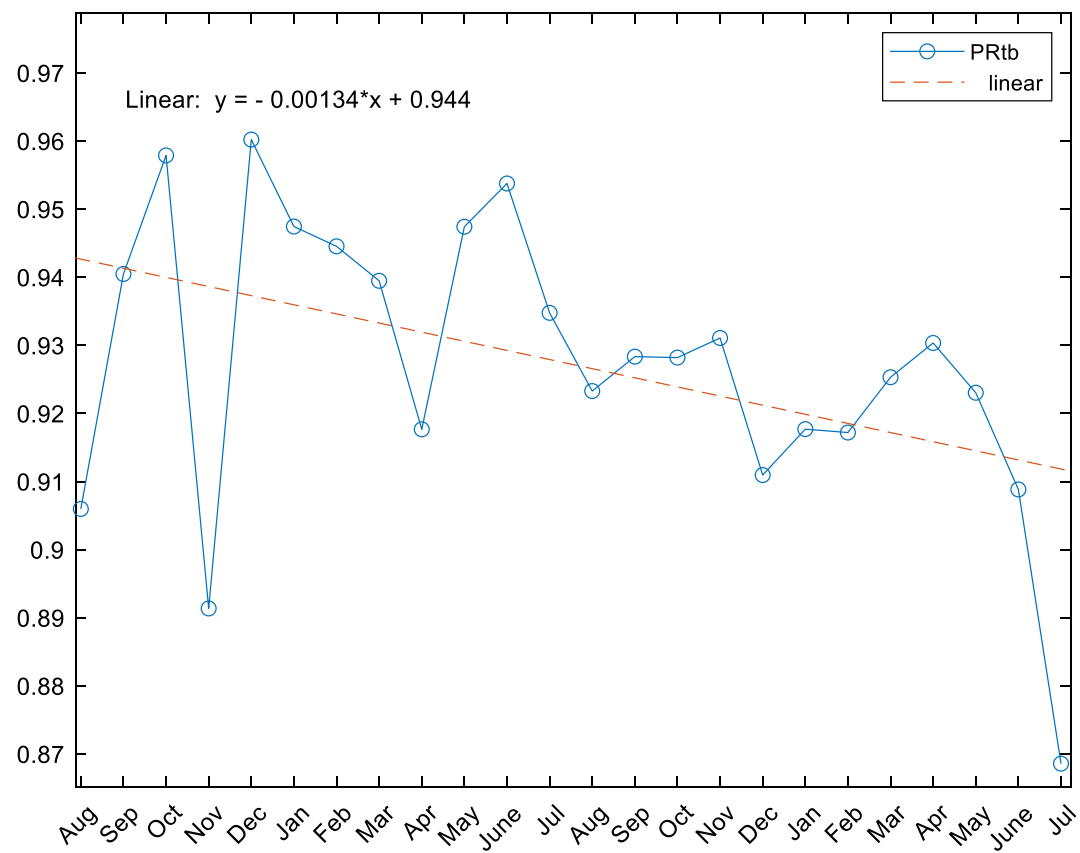
- More sensors both for Irradiance and for Temperature measurements

To use Eq. (4) and Eq. (5), which gave better results, in further studies it would be possible to use modeled, rather than measured, Temperature and rear Irradiance.

6. Conclusion

A simple method for calculating the Performance Loss Ratio was applied to a PV system equipped with bifacial PERC modules. The method has been divided into five steps, highlighting the critical issues in each phase of the application to data from a real plant. The simplicity of the method allows it to be replicated to other case studies. Longer datasets allow to obtain more reliable results on the PLR estimate due to the degradation effect, in particular when the annual degradation of the modules is low. The results of methodology used to estimate the PLR have been compared with the Power loss recorded through the Solar Simulator laboratory test.

The acquired electrical data used in the model are measured by a string of photovoltaic modules, so are included also losses due to sub-components and connections. All losses, except those that cause sudden and gross changes, are included in the PLR. The PLR represents an indicative tool for verifying the aging conditions of the modules, but not deterministic, the real uncertainty represents one of the critical issues on which the method can be improved. During the monitoring period of PV plants, extreme weather events, or even strong winds, hail and torrential rains, can occur. It is therefore important to take these events into account not just for the risk analysis of the PV plant before the installation phase but also in the evaluation of the PLR. The definition of limit values for environmental quantities such as wind and hail size/intensity could be a support for the evaluation of the PLR. In the case study, some hail

Fig. 17. Monthly PR_{Tb} and linear fitting, period Aug 2020–Jul 2022.**Table 4**

Summary monthly mean PR, PR_T and PR_{Tb} calculated within 800–1200 W/m² Irradiance filter, from Aug 2020 to July 2022.

Year	Month	Samples number (PR)	PR*	Samples number (PR _T)	PR _T *	Samples number (PR _{Tb})	PR _{Tb} *
2020	Aug	2370	0,91	1710	0,99	1853	0,91
	Sep	23	0,94	23	1,02	23	0,94
	Oct	4148	0,93	4121	1,03	4131	0,96
	Nov	3286	0,95	3257	0,95	3267	0,89
	Dec	3691	0,98	3667	1,03	3677	0,96
	Jan	2017	0,96	2000	1,03	2003	0,95
2021	Feb	6027	0,94	6007	1,02	6014	0,94
	Mar	5706	0,94	5670	1,01	5684	0,94
	Apr	5140	0,94	5112	1,01	5109	0,92
	May	4487	0,95	4459	1,03	4457	0,95
	June	5213	0,93	5194	1,03	5199	0,95
	Jul	6939	0,90	6927	1,01	6931	0,93
	Aug	7081	0,88	7066	0,99	7067	0,92
	Sep	6241	0,90	6179	1,00	6185	0,93
	Oct	3477	0,92	3421	1,00	3428	0,93
	Nov	2949	0,94	2905	1,02	2912	0,93
	Dec	4069	0,95	4048	1,00	4051	0,91
2022	Jan	4707	0,95	4666	1,00	4671	0,92
	Feb	6167	0,94	6125	0,99	6132	0,92
	Mar	4115	0,94	4043	1,00	4055	0,93
	Apr	4906	0,94	4877	1,00	4877	0,93
	May	6075	0,92	5981	0,99	5986	0,92
	June	4080	0,91	4070	0,98	4071	0,91
	Jul	7097	0,90	7069	0,94	7070	0,87

* The value of the monthly mean PR, PR_T and PR_{Tb} is approximated to the second significant digit exclusively in the table.

episodes occurred during the 2-year installation period, but since a dedicated sensor was not installed, it was not possible to assess its magnitude. Hail and wind can damage the modules depending on their

Table 5

PLR and uncertainty estimates for 2 years period, calculated using the monthly average of different metrics within 800–1200 W/m² Irradiance filter.

Metric	PLR [%]	u (PLR) [%]
PR	-3,21	1,72
PR _T	-3,85	1,52
PR _{Tb}	-3,41	1,46

magnitude but also depending on the photovoltaic technology and the quality of the PV module.

The PLR has been estimated by the “5-STEP method” using PR, PR_T and PR_{Tb} as metric, calculated within the narrow Irradiance range of 800/1200 W/m². The PR, PR_T and PR_{Tb} used as a metric for the monitored period, provided PLR values of -3.21 %, -3.85 and -3.41, which corresponds respectively to 1.65 %/y, 1.93 %/y and 1.71 %/y according to the linear interpolation over two years.

Finally, since the PV modules of the plant had been subjected to the solar simulator lab test after nineteen months of operation, recording the average Power decay of 3.35 %, it was possible to compare the PLR values that have been estimated with three different metrics and linear fitting, with the Power decay values associated exclusively with the PV modules.

Declaration of Competing Interest

The authors declare that they have no known competing financial interests or personal relationships that could have appeared to influence the work reported in this paper.

Acknowledgements

The authors want to thank Enel Green Power SpA for the doctoral fund of Gaetano Mannino, the technicians of Enel Green Power SpA for their availability.

This work is partially supported by Ministero dell'Istruzione, dell'Università e della Ricerca (Italy) (grant PRIN2020-HOTSPHOT 2020LB9TBC).

References

- Abdelouahed, A., Elmamoun, S., Berrada, A., Ameur, A., 2022. Photovoltaic modules degradation assessment using different statistical techniques. *Int. J. Energy Res.* 46, 116368.
- Belluardo, G., et al., 2015. Novel method for the improvement in the evaluation of outdoor performance loss rate in different PV technologies and comparison with two other methods. *Sol. Energy* 117, 139–152.
- Bouaichi, A., El Amrani, A., Ouhadou, M., Lfakir, A., Messaoudi, C., 2020. In-situ performance and degradation of three different photovoltaic module technologies installed in arid climate of Morocco. *Energy* 190, 116368.
- Bouraiou, A., Hamouda, M., Chaker, A., Lachtar, S., Neçaibia, A., Boutasseta, N., Mostefaoui, M., 2017. Experimental evaluation of the performance and degradation of single crystalline silicon photovoltaic modules in the Saharan environment. *Energy* 132, 22–30.
- Carigiet, F., Brabec, C.J., Baumgartner, F.P., 2021. Long-term power degradation analysis of crystalline silicon PV modules using indoor and outdoor measurement techniques. *Renew. Sustain. Energy Rev.* 144, 111005.
- da Silva, M.K., Gul, M.S., Chaudhry, H., 2021. Review on the sources of power loss in monofacial and bifacial photovoltaic technologies. *Energies* 14 (23), 7935.
- Gu, W., Ma, T., Ahmed, S., Zhang, Y., Peng, J., 2020. A comprehensive review and outlook of bifacial photovoltaic (BPV) technology. *Energy Convers. Manage.* 223, 113283. ISSN 0196-8904.
- GUM – JCGM 100, 2008, 2008. Evaluation of measurement data guide to the expression of uncertainty in measurement.
- IEC 61724-1:2021. Photovoltaic system performance - Part 1: Monitoring.
- JinkoSolar, 2020. Transparent backsheet vs dual glass—advantages and disadvantages [PV Tech [Online].
- Jordan, D.C., Deline, C., Kurtz, S.R., Kimball, G.M., Anderson, M., 2017. Robust PV degradation methodology and application. *IEEE J. Photovoltaics* 8 (2), 525–531.
- Jordan, D.C. et al., 2022. Photovoltaics module reliability for the terawatt age. *Prog. Energy*, 4, 022002.
- Jordan, D.C., Kurtz, S.R., 2013. Photovoltaic degradation rates—an analytical review. *Prog. Photovolt. Res. Appl.* 21 (1), 12–29.
- Kim, J., Rabelo, M., Padi, S.P., Yousuf, H., Cho, E.-C., Yi, J., 2021. A review of the degradation of photovoltaic modules for life expectancy. *Energies* 14, 4278. <https://doi.org/10.3390/en14144278>.
- King, D.L., Kratochvil, J.A., Boyson, W.E., 2004. Photovoltaic array performance model.
- Kopecek, R., Libal, J., 2021. Bifacial photovoltaics 2021: status. *Opprt. Challenges Energies* 14, 2076.
- Kunaifi, K., Reinders, A., Lindig, S., Jaeger, M., Moser, D., 2020. Operational performance and degradation of PV systems consisting of six technologies in three climates. *Appl. Sci.* 10 (16), 5412.
- Liang, T.S., Pravettoni, M., Deline, C., Stein, J.S., Kopecek, R., Singh, J.P., Khoo, Y.S., 2019. A review of crystalline silicon bifacial photovoltaic performance characterisation and simulation. *Energ. Environ. Sci.* 12 (1), 116–148.
- Lindig, S., Moser, D., Curran, A.J., Rath, K., Khalilnejad, A., French, R.H., Luo, W., 2021. International collaboration framework for the calculation of performance loss rates: data quality, benchmarks, and trends (towards a uniform methodology). *Prog. Photovolt. Res. Appl.* 29 (6), 573–602.
- Lindig, S., Theristis, M., Moser, D., 2022. Best practices for photovoltaic performance loss rate calculations. *Prog. Energy* 4 (2), 022003.
- Makrides, G., Zinsser, B., Georgiou, G.E., Schubert, M., Werner, J.H., 2010. Degradation of different photovoltaic technologies under field conditions. In: 2010 35th IEEE Photovoltaic Specialists Conference. p. 002332-002337. doi:10.1109/PVSC.2010.5614439.
- Piliougine, M., Oukaja, A., Sidrach-de-Cardona, M., Spagnuolo, G., 2021. Temperature coefficients of degraded crystalline silicon photovoltaic modules at outdoor conditions. *Prog. Photovolt. Res. Appl.* 29, 558–570. <https://doi.org/10.1002/pip.3396>.
- Quansah, D.A., Adaramola, M.S., 2019. Assessment of early degradation and performance loss in five co-located solar photovoltaic module technologies installed in Ghana using performance ratio time-series regression. *Renew. Energy* 131, 900–910.
- Romero-Fiances, I., et al., 2022. Impact of duration and missing data on the long-term photovoltaic degradation rate estimation. *Renew. Energy* 181, 738–748.
- Silvestre, S., Tahri, A., Tahri, F., Benlebna, S., Chouder, A., 2018. Evaluation of the performance and degradation of crystalline silicon-based photovoltaic modules in the Saharan environment. *Energy* 152, 57–63.
- Spataru, S.V., Gavriluta, A., Sera, D., Maaloe, L., Winther, O., 2016. Development and implementation of a PV performance monitoring system based on inverter measurements. In: 2016 IEEE Energy Conversion Congress and Exposition (ECCE). IEEE, pp. 1–7.
- Subramanyan, A.B., Pan, R., Kuitche, J., TamizhMani, G., 2018. Quantification of environmental effects on PV module degradation: a physics-based data-driven modeling method. *IEEE J. Photovoltaics* 8 (5), 1289–1296.
- Sulas-Kern, D.B., Owen-Bellini, M., Ndione, P., et al., 2021. Electrochemical degradation modes in bifacial silicon photovoltaic modules. *Prog. Photovolt. Res. Appl.* 1–11.
- Theristis, M., Stein, J.S., Deline, C., Jordan, D., Robinson, C., Sekulic, W., King, B.H., 2022. Onymous early-life performance degradation analysis of recent photovoltaic module technologies. *Prog. Photovolt. Res. Appl.*
- Tina, G.M., Cosentino, F., Ventura, C., 2016. Monitoring and diagnostics of photovoltaic power plants. In: *Renewable Energy in the Service of Mankind*, Vol. II. Springer, Cham, pp. 505–516.
- Tina, G.M., Scavo, F.B., Gagliano, A., 2020. Multilayer thermal model for evaluating the performances of monofacial and bifacial photovoltaic modules. *IEEE J. Photovoltaics* 10 (4), 1035–1043.
- VDMA, 2020. International Technology Roadmap for Photovoltaic (ITRPV).
- Wang, L.e., Tang, Y.i., Zhang, S.u., Wang, F., Wang, J., 2022. Energy yield analysis of different bifacial PV (photovoltaic) technologies: TOPCon, HJT, PERC in Hainan. *Sol. Energy* 238, 258–263.

Further reading

- www.solarbankability.org.
<https://it.mathworks.com/help/matlab/ref/rmoutliers.html>.